Supporting Information

Microscopic analysis of water/glycerol/EO30PS system in bulk and on a solid substrate

Makoto Uyama,* Roland Steitz,* Marcus Trapp, Laurence Noirez, Sebastian Bayer, and Michael Gradzielski*

*Corresponding authors: M.U.: makoto.uyama@shiseido.com

M.S.: steitz@helmholtz-berlin.de

M.G.: michael.gradzielski@tu-berlin.de

Number of Pages: 15
Number of Figures: 13

1. Polarization Microscopy

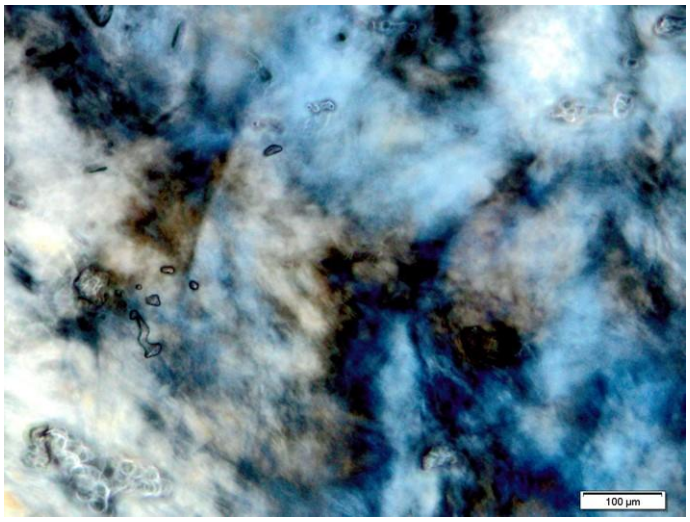

Figure S1. Polarized light microscopy image of water/glycerol/EO30PS = 30/10/60.

Figure S2. Polarized light microscopy image of water/glycerol/EO30PS = 60/10/30.

2. Dynamic Light Scattering (DLS)

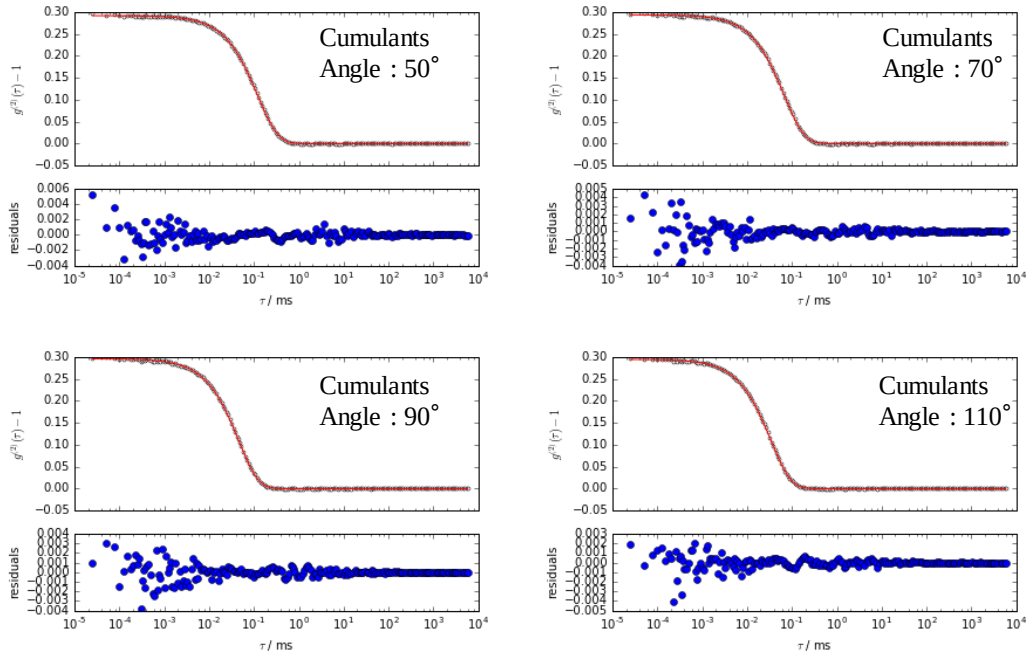

Figure S3. Autocorrelation functions (black lines) and cumulant fitting curves (red lines) obtained from water/glycerol/EO30PS = 85.5/9.5/5 at scattering angles 50, 70, 90, 110°.

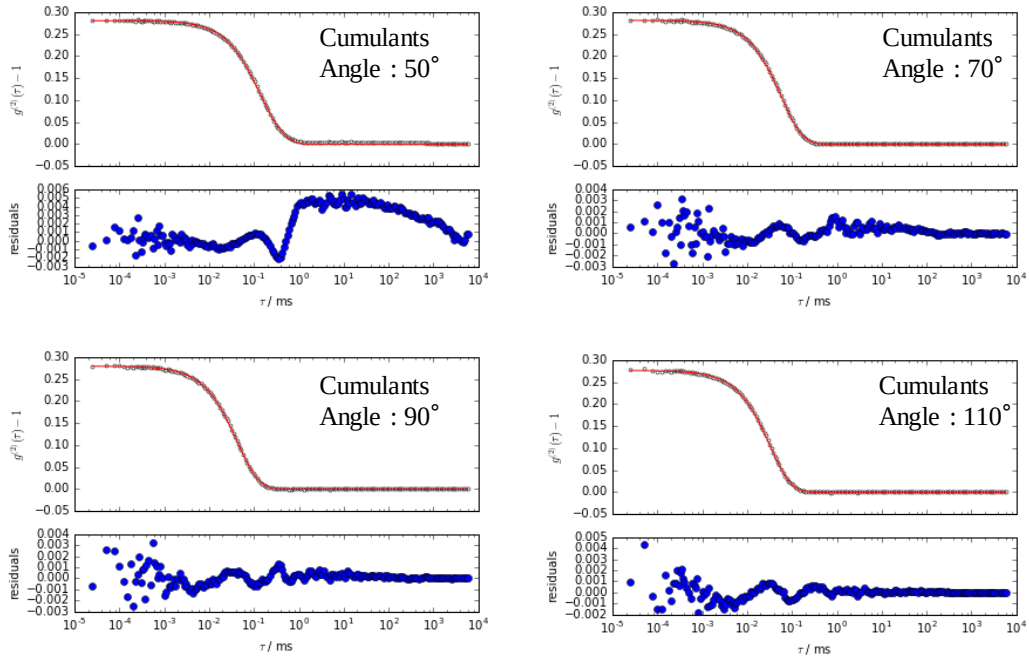

Figure S4. Autocorrelation functions (black lines) and cumulant fitting curves (red lines) obtained from water/glycerol/EO30PS = 72/18/10 at scattering angles 50, 70, 90, 110°.

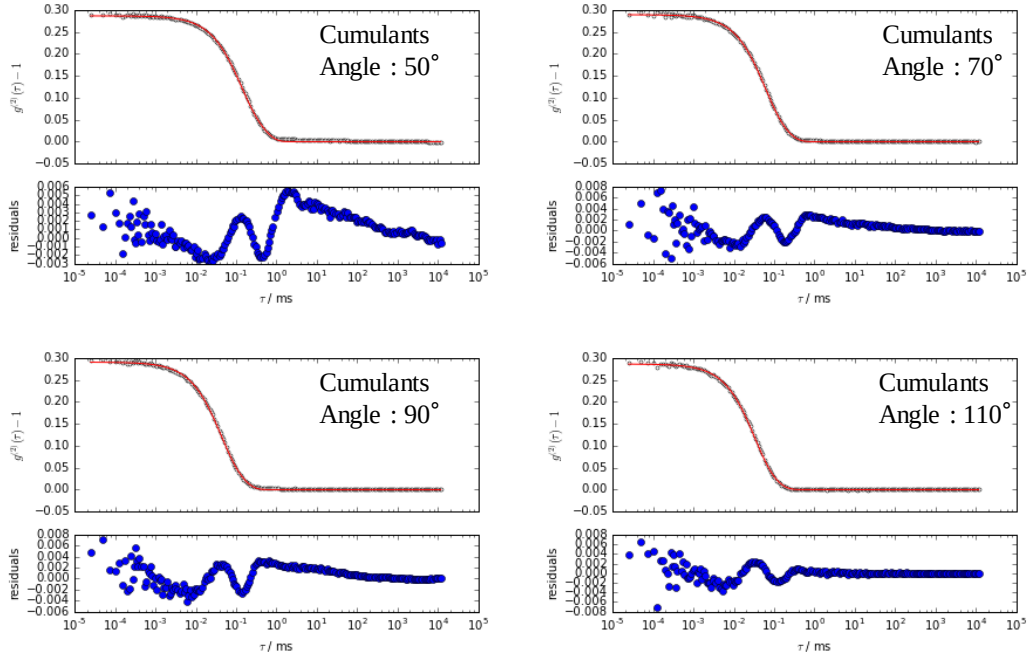

Figure S5. Autocorrelation functions (black lines) and cumulant fitting curves (red lines) obtained from water/glycerol/EO30PS = 59.5/25.5/15 at scattering angles 50, 70, 90, 110°.

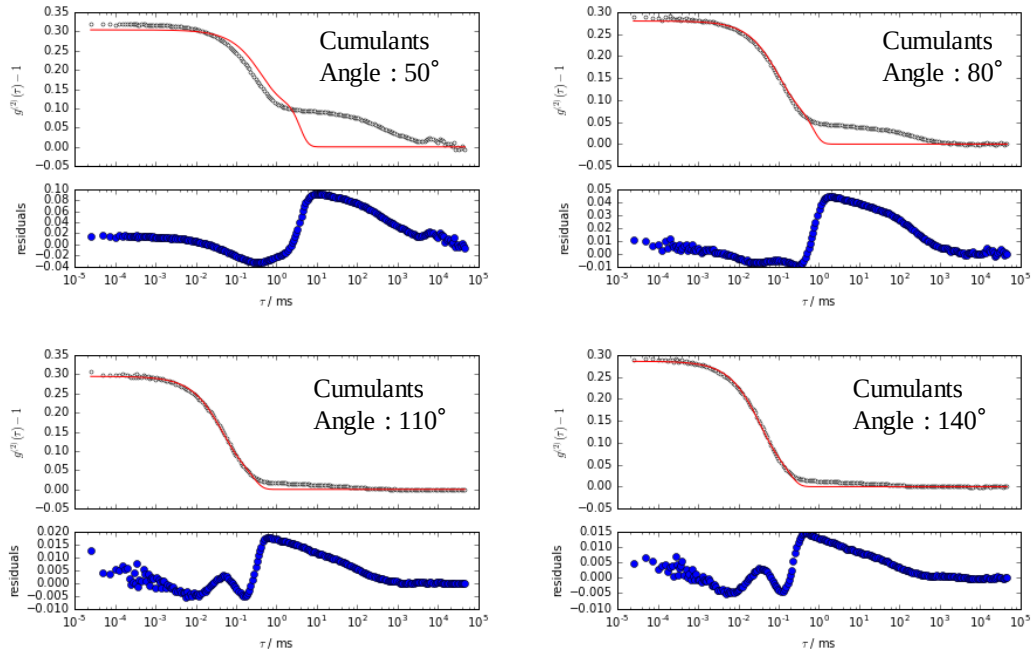

Figure S6. Autocorrelation functions (black lines) and cumulant fitting curves (red lines) obtained from water/glycerol/EO30PS = 48/32/20 at scattering angles 50, 80, 110, 140°.

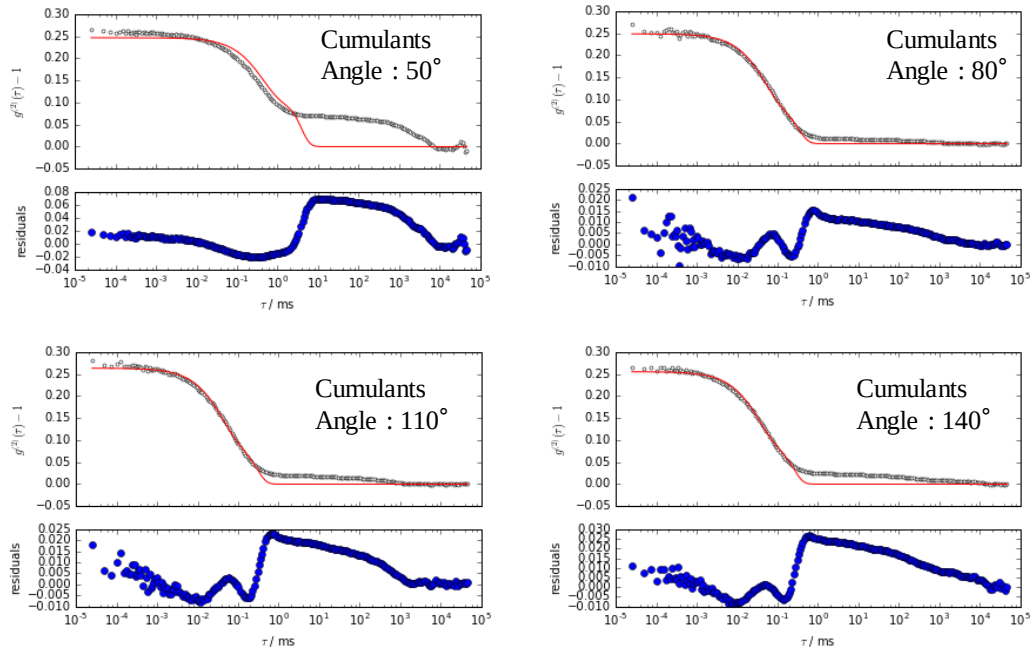

Figure S7. Autocorrelation functions (black lines) and cumulant fitting curves (red lines) obtained from water/glycerol/EO30PS = 37.5/37.5/25 at scattering angles 50, 80, 110, 140°.

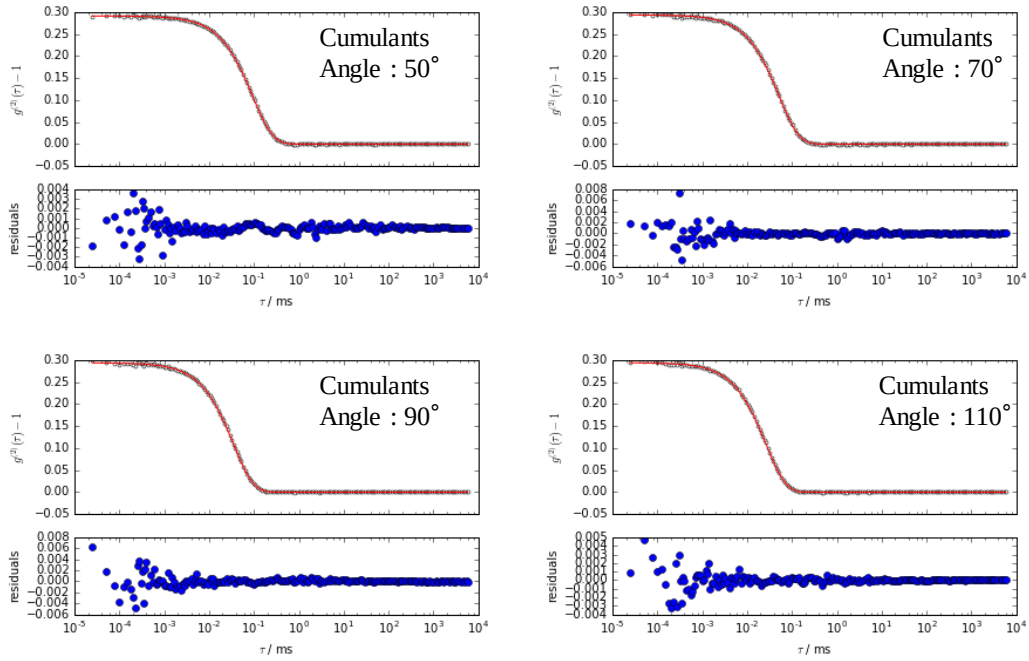

Figure S8. Autocorrelation functions (black lines) and cumulant fitting curves (red lines) obtained from water/EO30PS = 95/5 at scattering angles 50, 70, 90, 110°.

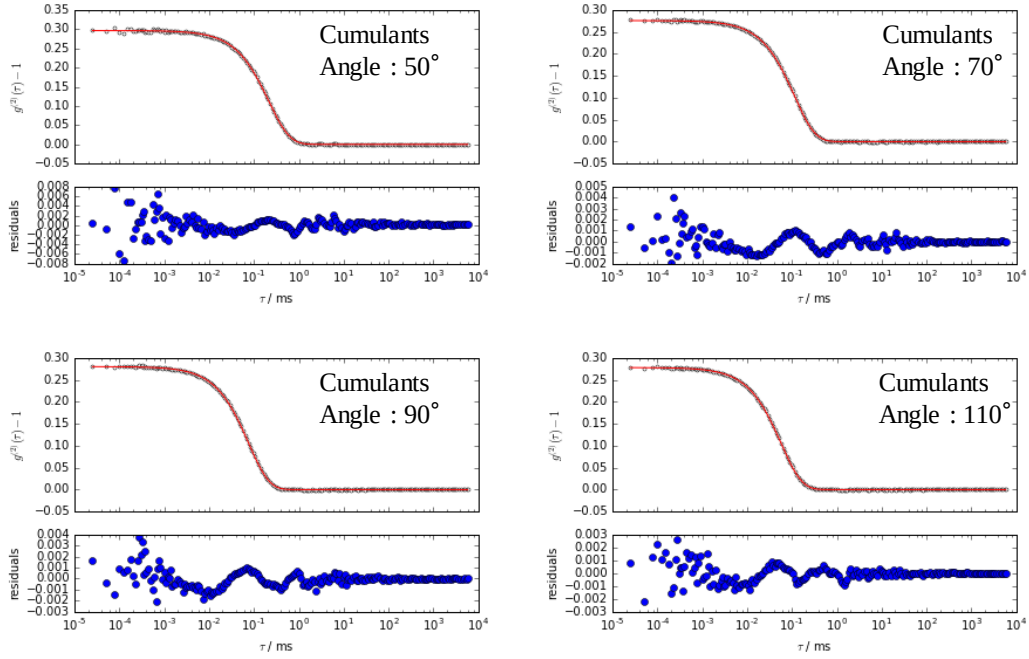

Figure S9. Autocorrelation functions (black lines) and cumulant fitting curves (red lines) obtained from water/glycerol/EO30PS = 66.5/28.5/5 at scattering angles 50, 70, 90, 110°.

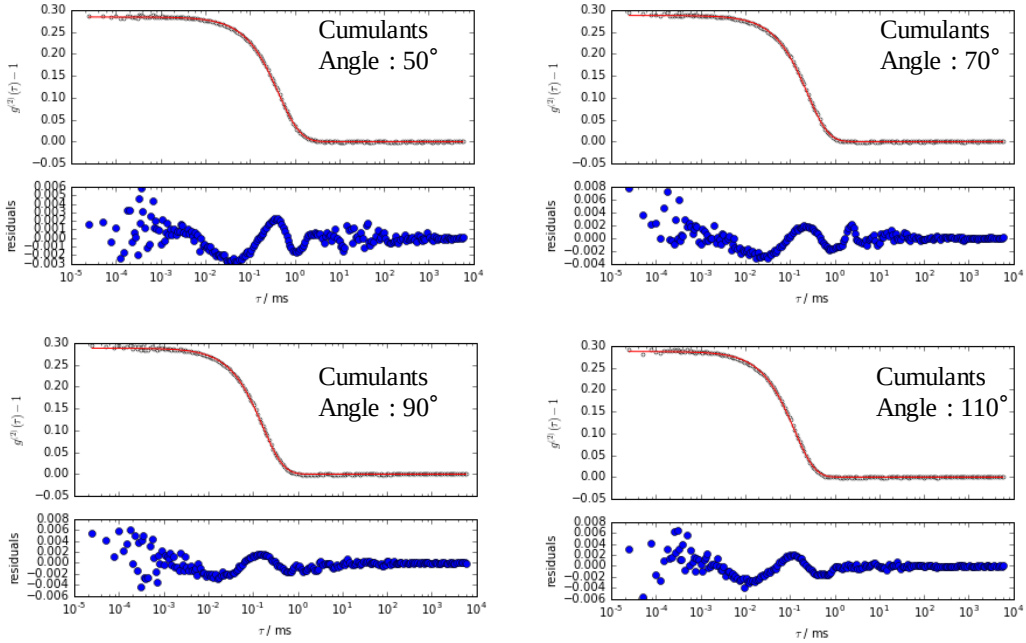

Figure S10. Autocorrelation functions (black lines) and cumulant fitting curves (red lines) obtained from water/glycerol/EO30PS = 47.5/47.5/5 at scattering angles 50, 70, 90, 110°.

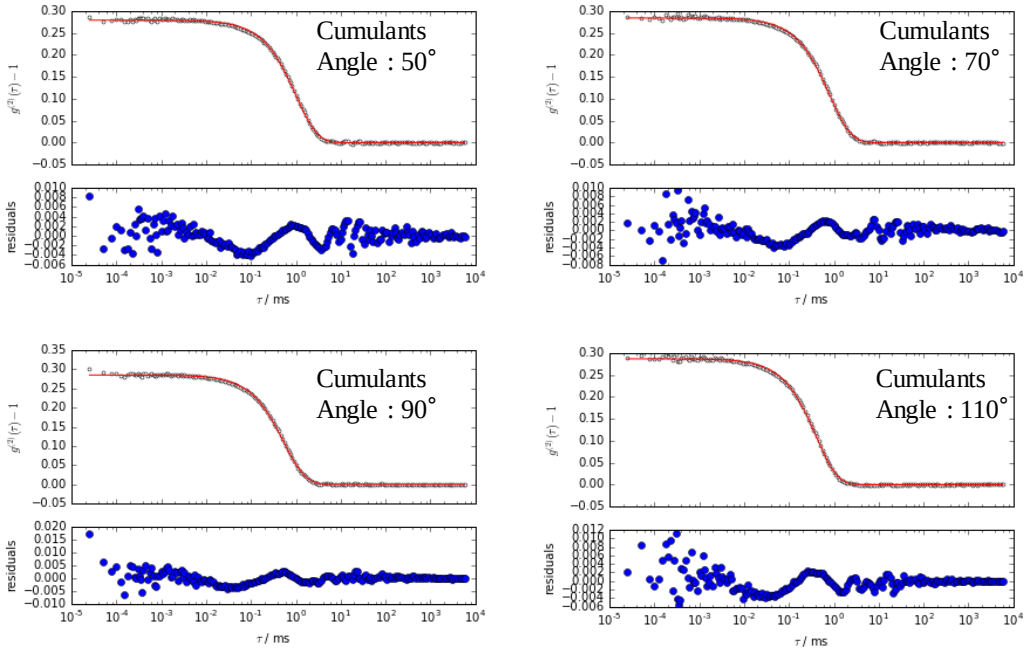

Figure S11. Autocorrelation functions (black lines) and cumulant fitting curves (red lines) obtained from water/glycerol/EO30PS = 28.5/66.5/5 at scattering angles 50, 70, 90, 110°.

3. Small-Angle Neutron Scattering (SANS)

A detailed analysis of the SANS data on absolute scale was performed with a self-written model for sasview 4.2.1 [1] with the analytical form factor F(q) of a monodisperse rotational ellipsoid [2, 3], interacting via hard-sphere interactions as described with the Percus-Yevick closure to the Ornstein-Zernicke equation [4] and yielding a hard sphere structure factor S(q).

The differential scattering cross section (absolute scattering intensity $I(q)$) with respect to the momentum transfer vector $d\sigma(q)/d\Omega$ for monodisperse particles and elastic scattering can be written as

$$\frac{d\sigma(q)}{d\Omega} = {}^{1}N\,F(q)^2 S(q) = \frac{\Phi}{V_p} F(q)^2 S(q) \qquad \text{(Eq. S1)}$$

Where ${}^{1}N$ is the number density and Φ the volume fraction of the scattering entity, V_p denotes the volume of the scattering particle, $F(q)$ denotes the particle form factor, which is the Fourier transform of the distribution of scattering mass in the particle, and $S(q)$ the structure factor, which describes the interactions between the particles.

For a homogeneous rotational ellipsoid, the form factor can be written as

$$F(q) = V_p \Delta\rho_{SL} \frac{3(\sin qr - qr\cos qr)}{(qr)^3} \qquad \text{(Eq. S2)}$$

$\Delta\rho_{SL}$ denotes the scattering contrast of the particle with respect to the solvent, and r is the ellipsoidal radius:

$$r = R_e(\sin^2\alpha + a^2\cos^2\alpha)^{1/2} \qquad \text{(Eq. S3)}$$

R_e denotes the equatorial radius of the ellipsoid, perpendicular to the rotational axis, a is

the axial ratio between the equatorial and the polar radius R_p/R_e, and α the angle between the axis of the ellipsoid and the scattering vector q. Since no anisotropic scattering signal was seen in the 2D detector images, we assumed no oriental ordering of the particles in the sample, for which the squared form factor is given by

$$\langle F(q)^2 \rangle = \int_0^{\pi/2} F(q,\alpha)^2 \sin\alpha \, d\alpha \qquad \text{(Eq. S4)}$$

$$I(q) = {}^1N\langle F(q)^2\rangle S(q) \qquad \text{(Eq. S5)}$$

For a monodisperse system, the inter-particle structure factor S(q) can be multiplied to yield the final scattering intensity, $I(q)$, according to Eq. S5. We assume no interaction potential for center-to-center distances larger than $2R_{HS}$ (hard sphere radius, R_{HS}), and an infinitely high repulsive interaction potential for smaller distances (hard sphere model). For an approximate analytical expression for this inter-particle structure factor, see e.g. [5].

To account for the fact that the hydrophilic poly(oxyethylene) part of the molecules is not assembled compactly, but dissolves well into the water-glycerol mixture, and that for the given concentrations the stretched length of the EO_{30}-PS molecules is longer than half of the center-to-center distance between two neighbouring micelles (as discussed below), two assumptions were made:

(I) The PEO part of the molecule is considered to be only partly part of the scattering spheroidal particle, the rest is considered to be homogeneously dissolved in the solvent. Therefore, a distribution parameter is introduced that describes the fraction of PEO that is part of the scattering particle in relation to the total volume fraction of PEO:

$$x_{PEO} = \frac{\Phi_{\text{PEO P}}}{\Phi\_\text{PEO}} \qquad \text{(Eq. S6)}$$

This factor is taken into account in a self-consistent manner for the scattering contrast calculation and the volume fraction of the scattering particle.

(II) Due to the outreaching character of the PEO chains, the interaction between the particles starts already before close contact with the scattering particle we just defined. This is accounted for by an effective hard sphere interaction radius R_{HS} which is slightly larger than the radius that would arise from a sphere with the scattering volume used for the form factor calculation, which does not include any hydration water (see table). The effective volume fraction of the interacting particles Φ_{HS} is therefore larger by a factor $\chi_{HS} = V_{HS}/V_p$.

With these assumptions, the scattering contrast $\Delta\rho_{SL}$ as well as the volume fraction of the scattering particles Φ were calculated from the composition and the scattering length densities (given in Table S1) of the pure compounds according to the following formulas (the sample compositions are summarized in Table S2):

$$\Phi = \Phi_{PS} + \chi_{PEO}\Phi_{PEO} \quad \text{(Eq. S7)}$$

$$\rho_{SL\,P} = \frac{\Phi_{PS}\rho_{SL\,PS} + x_{PEO}\Phi_{PEO}\rho_{SL\,PEO}}{\Phi} \quad \text{(Eq. S8)}$$

$$\rho_{SL\,sol} = \frac{\Phi_{D2O}\rho_{SL\,D2O} + \Phi_{gly}\rho_{SL\,gly} + (1 - x_{PEO})\Phi_{PEO}\rho_{SL\,PEO}}{1 - \Phi} \quad \text{(Eq. S9)}$$

$$\Delta\rho_{SL} = \rho_{SLP} - \rho_{SLsol} \quad \text{(Eq. S10)}$$

The indices *PS*, *PEO*, *gly* and *D2O* denote the phytosterol and poly(oxy ethylene) part of the surfactant molecule, glycerol and D_2O, respectively. *P* denotes particle, and *sol* the solvent.

Based on the particle volume V_p and the axial ratio a, the two radii can be calculated based

on the following formulas:

$$R_e = \sqrt[3]{\frac{3}{4\pi}\frac{V_p}{a}} \qquad \text{(Eq. S11)}$$

$$R_a = R_e a \qquad \text{(Eq. S12)}$$

The parameters obtained from applying this model to the experimental data are summarized in Table S3.

Table S1. Molecular weight (M_w), density (ρ), and scattering length density (ρ_{SL}) for the components contained.

	M_w	ρ	ρ_{SL}
	g/cm^3	g/mol	10^{-4}/nm^2
D_2O	20.03	1.11	6.36
glycerol	92.09	1.26	0.61
EO_{30}	1337	1.14	0.65
PS	399	1.05	0.032

Table S2. Detailed sample composition (water/glycerol/EO30PS) of the samples studied by SANS, given in terms of the volume fractions.

composition	Φ_{D2O}	Φ_{gly}	Φ_{EO}	Φ_{PS}
85.5/9.5/5	0.877	0.077	0.035	0.011
72/18/10	0.756	0.150	0.071	0.023
59.5/25.5/15	0.639	0.217	0.109	0.035
48/32/20	0.526	0.278	0.148	0.048
37.5/37.5/25	0.418	0.332	0.189	0.061

Table S3. Parameters derived from the SANS analysis for the different samples (composition: water/glycerol/EO30PS).

composition	$\Delta\rho_{SL}$ $10^{-4}/nm^2$	V_p nm^3	a	Φ_{HS}	^1N nm^{-3}
85.5/9.5/5	-5.42	240	0.45	0.116	9.59E-05
72/18/10	-4.82	180	0.45	0.237	2.66E-04
59.5/25.5/15	-4.22	155	0.45	0.329	4.38E-04
48/32/20	-3.62	135	0.42	0.367	6.19E-04
37.5/37.5/25	-3.02	135	0.38	0.395	7.60E-04

4. Neutron Reflectometry (NR)

An important question arising for the analysis of the NR data is to which extent it might be compromised by the effect of also seeing some bulk scattering. For this purpose, we did some simulation of the expected effect on the bulk scattering on the NR curves. As shown in Figure S11 not only the peak position is matching well, but especially the expected maximum intensity of the peak arising from bulk scattering is much less than that observed experimentally in the NR data. Accordingly, one can exclude that the effect of bulk scattering plays a major role here.

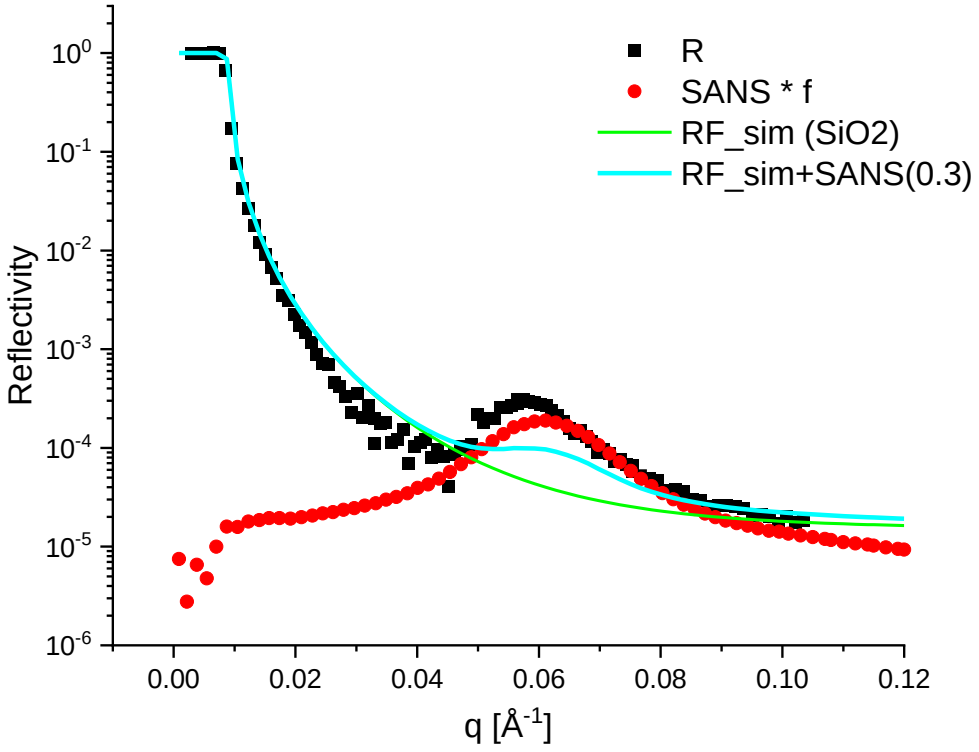

Figure S12. NR curve for D_2O/glycerol/EO30PS = 48/32/20 system., which is compared to the expected data from the pure substrate (green) and the one expected with the bulk scattering (blue) included.

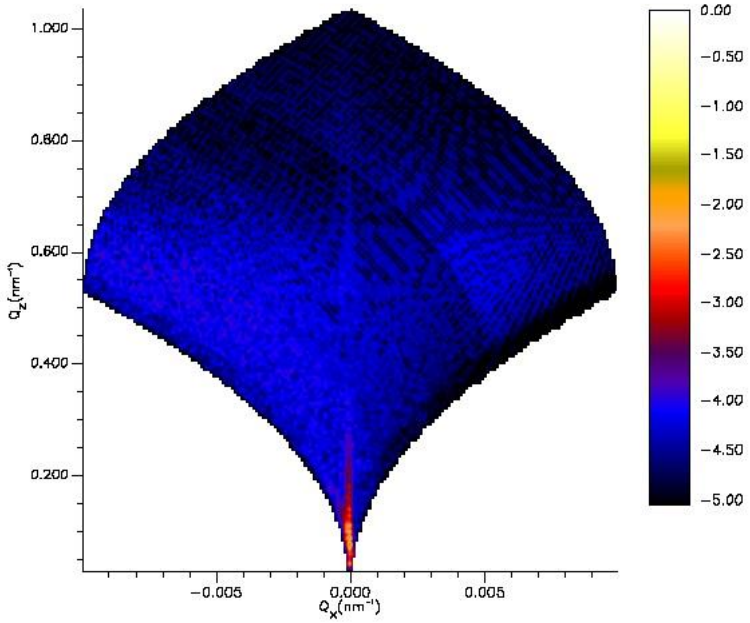

Figure S13. The Q_x vs Q_z map for D_2O/glycerol/EO30PS = 48/32/20 solution at 25 °C.

References:

[1] M. Doucet, et al. SasView Version 4.2, http://doi.org/10.5281/zenodo.1412041

[2] A Guinier. La Diffraction Des Rayons X Aux Très Petits Angles: Application À L'étude De Phénomènes Ultramicroscopiques. Annales de physique, **1939,** 11(12): 161–237.

[3] A. L. Patterson. The Diffraction of X-Rays by small Crystalline Particles. *Phys. Rev.* **1939,** 56: 972–977.

[4] J. K. Percus, G. J. Yevick, Analysis of Classical Statistical Mechanics by Means of Collective Coordinates. *Phys. Rev.* **1958,** 110, 1, doi:10.1103/PhysRev.110.1

[5] N. W. Ashcroft, J. Lekner, Structure and Resistivity of Liquid Metals, *Phys. Rev.* **1966**, *145*, 83-90.